



OPEN ACCESS

EDITED BY

Emilia Vitale,
National Research Council (CNR), Italy

REVIEWED BY

Cheng Ni,
Chinese Academy of Medical Sciences
and Peking Union Medical College, China
Hongtao Qin,
Hunan University, China

*CORRESPONDENCE

Alexander M. van der Linden
✉ avanderlinden@unr.edu

RECEIVED 12 July 2024

ACCEPTED 10 March 2025

PUBLISHED 24 March 2025

CITATION

Alshareef HZ, Ballinger T, Rojas E and
van der Linden AM (2025) Loss
of age-accumulated *crh-1* circRNAs
ameliorate amyloid β -induced toxicity in a
C. elegans model for Alzheimer's disease.
Front. Aging Neurosci. 17:1464015.
doi: 10.3389/fnagi.2025.1464015

COPYRIGHT

© 2025 Alshareef, Ballinger, Rojas and van
der Linden. This is an open-access article
distributed under the terms of the [Creative
Commons Attribution License \(CC BY\)](#). The
use, distribution or reproduction in other
forums is permitted, provided the original
author(s) and the copyright owner(s) are
credited and that the original publication in
this journal is cited, in accordance with
accepted academic practice. No use,
distribution or reproduction is permitted
which does not comply with these terms.

Loss of age-accumulated *crh-1* circRNAs ameliorate amyloid β -induced toxicity in a *C. elegans* model for Alzheimer's disease

Hussam Z. Alshareef, Thomas Ballinger, Everett Rojas and
Alexander M. van der Linden*

Department of Biology, University of Nevada, Reno, NV, United States

Circular RNAs (circRNAs) are non-coding RNAs mostly derived from exons of protein-coding genes via a back-splicing process. The expression of hundreds of circRNAs accumulates during healthy aging and is associated with Alzheimer's disease (AD), which is characterized by the accumulation of amyloid-beta ($A\beta$) proteins. In *C. elegans*, many circRNAs were previously found to accumulate during aging, with loss of age-accumulated circRNAs derived from the CREB gene (*circ-crh-1*) to increase mean lifespan. Here, we used *C. elegans* to study the effects of age-accumulated circRNAs on the age-related onset of $A\beta$ -toxicity. We found that *circ-crh-1* mutations delayed $A\beta$ -induced muscle paralysis and lifespan phenotypes in a transgenic *C. elegans* strain expressing a full-length human $A\beta$ -peptide ($A\beta_{1-42}$) selectively in muscle cells (GMC101). The delayed $A\beta$ phenotypic defects were associated with the inhibition of $A\beta$ aggregate deposition, and thus, genetic removal of *circ-crh-1* alleviated $A\beta$ -induced toxicity. Consistent with a detrimental role for age-accumulated circRNAs in AD, the expression level of *circ-crh-1* expression is elevated after induction of $A\beta$ during aging, whereas linear *crh-1* mRNA expression remains unchanged. Finally, we found that the delayed onset of $A\beta$ -induced paralysis observed in *circ-crh-1* mutants is dependent on the *col-49* collagen gene. Taken together, our results show that the loss of an age-accumulated circRNA exerts a protective role on $A\beta$ -induced toxicity, demonstrating the utility of *C. elegans* for studying circRNAs in AD and its relationship to aging.

KEYWORDS

Alzheimer's disease model, $A\beta_{1-42}$, *crh-1*, CREB, circular RNA, collagen, *C. elegans*, aging

1 Introduction

Circular RNAs (circRNAs) emerged as an intriguing class of non-coding RNAs with unique closed-loop structures. CircRNAs are generated through a process known as back-splicing during conventional RNA splicing, where the 3' and 5' ends of a pre-mRNA molecule are covalently bonded, yielding a circular configuration (Li et al., 2018). Most identified circRNAs are produced from exons of protein-coding genes (Zhang et al., 2014). Their lack of free ends confers circRNAs a degree of resistance to exoribonuclease digestion compared to their linear counterparts (Jeck et al., 2013), which can contribute to their

stability and abundance. Despite these characteristics, the functions of many circRNAs remain largely elusive, although their functions appear to be intertwined with the molecules they interact with.

CircRNAs accumulate during the normal process of aging in *C. elegans* (Cortés-López et al., 2018), *Drosophila* (Westholm et al., 2014; Hall et al., 2017), and mice (Gruner et al., 2016) and are found to play both positive and negative roles in the aging of *C. elegans*, *Drosophila*, and various mammalian tissues (Knupp and Miura, 2018; Kim et al., 2021). Prominent examples include the extension of lifespan through *circSfl* transgenic overexpression in *Drosophila* (Weigelt et al., 2020) and the loss of the circRNA derived from the host gene *crh-1/CREB* in *C. elegans* (Knupp et al., 2022). Additionally, growing evidence suggests key roles of circRNAs in Alzheimer's disease (AD) by affecting mechanisms such as neuroinflammation, oxidative stress and autophagy, as well as amyloid-beta (A β) production and degradation (Beylerli et al., 2024). For example, circular RNA *ciRS-7* (also known as *CDRIas*) inhibits the activity of microRNA, *mir-7* (Hansen et al., 2013), which subsequently effects the accumulation of A β plaques in AD (Shi et al., 2017; Sun et al., 2023). Considering that brain aging is highly associated with AD pathogenesis, circRNAs that accumulate with aging may also contribute to AD. CircRNAs can act as molecular sponges, sequestering microRNAs (miRNAs) (Hansen et al., 2013; Zhang et al., 2020) and RNA-binding proteins (RBPs) (Patop et al., 2019; Chen, 2020) away from their messenger RNA (mRNA) targets, thereby altering the splicing or expression patterns of these mRNAs. However, our understanding of the functional roles of age-accumulated circRNAs in AD remains limited.

C. elegans presents a powerful model organism for studying age-associated circRNAs in AD. Previously, we demonstrated that a majority of circRNAs expressed in *C. elegans* accumulate during aging (Cortés-López et al., 2018). Using CRISPR/Cas9, we genetically removed two abundant age-accumulated circRNAs derived from the *crh-1* gene (*circ-crh-1*), which encodes the homolog of CREB, without disrupting the linear RNA and its associated activated protein (Knupp et al., 2022). The genetic loss of this age-accumulated *circ-crh-1* extended the mean lifespan of *C. elegans* (Knupp et al., 2022), suggesting that *circ-crh-1* abundance might contribute to age-related decline. Here, we extend our findings by testing the impact of *circ-crh-1* removal on a severe model of inducible amyloidosis in *C. elegans*. We used the transgenic *C. elegans* strain (GMC101), which expresses human A β_{1-42} peptides constitutively in muscle cells that mimics the pathological features of AD (McCull et al., 2012). We found that the loss of *circ-crh-1* expression delayed A β -induced paralysis of GMC101, improved its shortened mean lifespan, and reduced A β aggregate formation. Moreover, *circ-crh-1*(-) mutants exhibited an increase in the expression of the *col-49* collagen gene. Mutations in *col-49* exacerbated A β -induced paralysis, while *col-49* overexpression reduced paralysis induced by A β . Further investigation revealed that the delayed onset of A β -induced paralysis observed in *circ-crh-1*(-) mutants is dependent on *col-49* expression. Together, our results show that loss of age-accumulated *chr-1* circRNAs increase the

expression of the *col-49* collagen gene, thereby reducing A β -induced toxicity in a *C. elegans* transgenic model for Alzheimer's disease.

2 Materials and methods

2.1 Strains, general animal cultivation and genetic controls

Worms were cultivated on the surface of NGM agar seeded with the *Escherichia coli* strain OP50 as the primary food source and grown in 20°C incubators using standard protocols unless indicated otherwise. All experiments were performed on hermaphrodites. The wild-type strain N2, variety Bristol (Brenner, 1974) and other strains used in this study are listed in Supplementary Table 1. Strains were constructed using standard genetic methods (Fay, 2006) and genotypes were confirmed either by phenotype (for example, the transgenic strain was marked by fluorescence) or by PCR (for example, by identifying small deletions in mutant strains).

2.2 Generation of plasmids, transgenic animals, and *col-49* mutants

To generate transgenic worms expressing the *circ-crh-1* in muscle cells, exon 4 of *crh-1* and intronic sequences flanking exon 4 (Figure 4A) were cloned into the pMC10 plasmid (a kind gift from the Sengupta Lab). Next, promoter sequences of *myo-3* (~2.5 kb) were cloned at the 5'-end of the *circ-crh-1* sequence using the multi cloning site (MCS) of pMC10. The generated *myo-3p::circ-crh-1* construct along with the *unc-122p::RFP* co-injection marker (AddGene) was injected into VDL1300 *crh-1*(*syb385*); *dvIs100*[*unc-54p::A β_{1-42} ::unc-54 3'-UTR, mtl-2p::GFP*] animals to create the VD12 strain. Transgenic worms carrying extrachromosomal arrays overexpressing *pie-1p::circ-crh-1* (VDL975), *rab-3p::circ-crh-1* (VDL1104) were crossed with the VDL1300 strain to create VDL1306 and VDL1307 strains (Supplementary Table 1). A *col-49* mutant allele (*syb8747*) harboring a 1180bp deletion was generated using a Co-CRISPR method to create the VD10 strain (SunnyBiotech), which was confirmed by PCR and Sanger sequencing. sgRNAs used to generate the *col-49*(*syb8747*) mutant were Sg1: 5'-cctcatcatcatgtggaattcg and Sg2: 5'-cccacttagaactgcttgattcg. We crossed the VD10 with the GMC101 strain to create VDL1308 *col-49*(*syb8747*); *dvIs100*[*unc-54p::A β_{1-42} ::unc-54 3'-UTR, mtl-2p::GFP*]. We then crossed the VDL1308 with the VDL1300 strain to create VDL1310 *crh-1*(*syb385*); *col-49*(*syb8747*); *dvIs100*[*unc-54p::A β_{1-42} ::unc-54 3'-UTR, mtl-2p::GFP*] using standard genetic methods. We generated a transgenic line that overexpresses *col-49* from a transgene carrying a multiple copy array of the *col-49* genomic sequence (~1.2 kb) under control of its endogenous promoter upstream sequence (~2 kb) and *col-49* 3'-UTR sequence (~1 kb). The resulting plasmid (*col-49p::col-49 genomic::col-49 3'-UTR*) along with the *unc-122p::RFP* co-injection marker was injected into wild-type worms to generate VD16 (SunnyBiotech). Next, we crossed the

VD16 with the GMC101 strain to create the VDL1309 strain using standard genetic methods. [Supplementary Table 1](#) shows all strains created and used in this study.

2.3 Lifespan analysis

All strains were maintained at 20°C for at least two generations before the lifespan assay. Adult worms age-synchronized by hypochlorite treatment and collected eggs were hatched overnight at 20°C. L1 larvae were then plated onto NGM plates seeded with *E. coli* OP50 bacteria. At the L4 larval stage, 90–150 worms per genotype were transferred to new 6 cm NGM plates seeded with 10x concentrated *E. coli* OP50 bacteria containing 0.5 μM 5-fluorodeoxyuridine (FUdR) to inhibit the development of self-progeny, and then shifted at the young adult stage to 25°C. Each strain was assayed in parallel and each plate contained 10–15 worms. Worms were blindly scored every day and were considered dead when they did not respond to touch of the platinum wire pick and were subsequently removed from the plate. Worms that experienced ventral rupture, bagging, or walling were censored from the lifespan analysis.

2.4 Paralysis assays

The paralysis assay was performed using GMC101 transgenic animals expressing *unc-54p::Aβ_{1–42}* as described previously ([McColl et al., 2012](#)). Briefly, worms were age-synchronized by hypochlorite bleaching and cultivated at 20°C. After they reached the L4 larval stage, worms were transferred to assay plates freshly seeded with *E. coli* OP50 bacteria, containing 0.5 μM of FUdR to inhibit the development of self-progeny, and then shifted at the young adult stage to the higher permissive 25°C temperature to induce paralysis unless indicated otherwise. About 15 worms were placed on each 6 cm NGM plate, and animals were blindly scored every 24 h as “paralyzed” if they failed to perform a full body wave propagation following a repeated touch-provoked response.

2.5 Total RNA collection and extraction

Worms were age-synchronized worms by hypochlorite treatment and collected eggs were hatched overnight at 20°C in 1x M9 buffer. L1 larvae were then plated onto NGM plates seeded 10x concentrated *E. coli* OP50 bacteria and allowed to develop to the L4 larval stage at 20°C. L4 larvae were then collected, washed and re-plated onto *E. coli* OP50 seeded NGM plates containing 0.5 μM FUdR. Worms were either upshifted to 25°C or kept at 20°C. Adult worms were collected at different aging time-points and washed with 1x M9 buffer through 35 μM nylon mesh to remove bacteria. Worm pellets of 100–300 μl were then transferred into green RINO tubes (Next Advance) and TRizol LS reagent (ThermoFisher Scientific, Cat #10296028) was added in a 1:3 ratio. Worms were immediately lysed by bead beating them for 5 min using a Bullet Blender Pro Storm (Next Advance). Total RNA was extracted using the Purelink RNA mini-kit, followed by a DNase I treatment following the manufacturer’s protocol (Ambion, Cat

#12183020). RNA was quantified by a Nanodrop. Bioanalyzer or tapestation (Agilent) were used for qualification as needed, and samples were stored at –80°C.

2.6 Analysis by RT-qPCR

To quantify and confirm individual circular or linear transcripts, 0.5 μg total RNA was reverse transcribed using Superscript III to prepare cDNA using random hexamers (Invitrogen, Cat #18080051). Next, cDNA samples were diluted and used with PowerUp SYBR Green Master Mix (Applied Biosystems, Cat #A25471) for RT-qPCR analysis analyzed on a CFX96 Real-Time System (Bio-Rad). For RT-qPCRs of circRNAs, we used outward-facing primers. For host gene linear RNA counterparts, one primer was located in the circularizing exon and the other was located in the upstream or downstream non-circularizing exon. For linear mRNAs such as collagen-encoding genes and Aβ mRNA, we used forward-facing primers. Fold-change values were calculated using wild-type (N2) ΔCt as control values for the $2^{-\Delta\Delta Ct}$ method. Data is normalized to housekeeping genes (*cdc-42* or *act-1*) mRNA. Primer sequences are listed in [Supplementary Table 2](#).

2.7 Imaging and quantification of Aβ aggregates in living animals

Four-day old adults were randomly collected during paralysis assays and stained with 1 mM X-34 (Sigma, Cat # SML1954) 10 mM Tris-HCl pH 8.0 for 2 h as previously described ([Link et al., 2001](#)). Stained worms were then washed twice with 1x M9 and transferred to *E. coli* seeded NGM plates containing 0.5 μM FUdR for 24 h to de-stain worms. De-stained 5-day old adults were then placed onto a 2% agarose pad with 10 μM levamisole to anesthetize worms. Confocal microscopy was used to acquire and capture images of the worm head using a 40x oil objective (405 nm excitation, 470–520 nm emission range). ImageJ software (NIH) was used to quantify Aβ aggregates.

2.8 Total collagen level determination

As previously described ([Teuscher et al., 2019](#)), worms were age-synchronized by hypochlorite treatment and collected eggs were hatched overnight at 15°C, 20°C, or 25°C in 1x M9 buffer. L1 larvae were then plated onto NGM plates seeded *E. coli* OP50 bacteria and allowed to develop 24 h post-L4 larval stage (1-day adult) at 15°C, 20°C, or 25°C. 1-day adult worms were then collected with 1x M9 buffer and washed with dH₂O through a 35 μM nylon mesh to remove bacteria. Worm pellets of 300 μl were then transferred into green RINO tubes (Next Advance) and lysed by bead beating them for 10 min using a Bullet Blender Pro Storm (Next Advance). Total collagen level was determined using the QuickZyme Total Collagen Kit (QuickZyme Biosciences), following the manufacturer’s protocol. Briefly, lysate samples were mixed with 12M HCl solution and incubated for 20 h at 95°C. Then assay buffer was added, and the 96-well plate was incubated at room temperature for 20 min, followed by the addition of the

detecting reagent and incubation at 60°C for 60 min. Total collagen level was measured and quantified as a fraction of total protein abundance using a Synergy HT BioTek microplate reader. Total protein levels were quantified using the PierceTM BCA Protein Assay Kit (ThermoFisher Scientific) following the manufacturer's protocol.

2.9 Statistical analysis

Statistical comparisons and graphical representations were performed with the Online Application for Survival Analysis, OASIS 2 (Han et al., 2016). For lifespan survival and paralysis curves, we used the Mantel-Cox log-rank test. Other data were analyzed using Graphpad Prism 9 software and statistical comparisons made include the Mann-Whitney *t*-test or the one-way ANOVA followed by a *post hoc* multiple-comparisons test. *p*-values are reported in the figure legends.

3 Results

3.1 circ-*crh-1* mutants delay the onset of A β -induced paralysis

We previously demonstrated that expression of circ-*crh-1* accumulates with *C. elegans* aging (Cortés-López et al., 2018) and that loss of circ-*crh-1* expression results in a significant extension of mean lifespan (Knupp et al., 2022). To directly test whether circ-*crh-1* expression plays a role in A β -induced toxicity, we used the GMC101 strain (further referred as *unc-54p::A β ₁₋₄₂*) in which expression of human A β ₁₋₄₂ peptides constitutively in muscle cells provokes an inducible age-progressive full-body paralysis when shifted from the non-restrictive 20°C temperature to a higher permissive 25°C temperature (McColl et al., 2012). We observed that mutations in circ-*crh-1* (*syb385* and *syb2657*), which exhibit a complete loss of circ-*crh-1* expression but normal linear *crh-1* expression, showed less severe paralysis in *unc-54p::A β ₁₋₄₂* animals at the higher permissive 25°C temperature (Figure 1A; Knupp et al., 2022). Thus, loss of circ-*crh-1* expression significantly delayed the onset of A β -induced paralysis.

3.2 circ-*crh-1* mutants reduce A β -induced lifespan shortening

To further test the protective effect of circ-*crh-1* expression A β -induced toxicity, we next tested its loss on the lifespan of *unc-54p::A β ₁₋₄₂* expressing animals. Previous work has shown that the expression of A β ₁₋₄₂ in body wall muscle cells severely decreased lifespan (Gallrein et al., 2021). Similarly, we found that *unc-54p::A β ₁₋₄₂* expressing animals led to a significantly shorter mean lifespan compared to wild-type controls (20.5% reduction, 8.10 days for GMC101 versus 10.19 days for wild-type, *p* < 0.0001) when animals were shifted from 20°C to the higher permissive 25°C temperature (Figure 1B). Interestingly, *crh-1(syb385)* was able to restore the reduced lifespan of *unc-54::A β ₁₋₄₂*

animals back to wild-type levels (9.7 days for *crh-1(syb385); unc-54::A β ₁₋₄₂* versus 8.1 days for GMC101, *p* < 0.0001) (Figure 1B). No significant differences were observed in mean lifespan between *unc-54::A β ₁₋₄₂* and wild-type animals (*p* = 0.614) at the 20°C temperature (no A β -induction) (Supplementary Figure 1). Thus, circ-*crh-1* mutations prevented lifespan shortening induced by A β . Together, these findings suggest that loss of circ-*crh-1* expression protects *C. elegans* from A β -induced toxicity.

3.3 circ-*crh-1* expression is increased following A β -induction

We next examined the impact of A β -induction on the expression of the age-accumulated circ-*crh-1* in aged *unc-54::A β ₁₋₄₂* animals compared to wild-type. We therefore conducted RT-qPCR analysis to measure the RNA fold change of circ-*crh-1* expression (i.e., *cel-circ_0000439*) in 4-day old adults compared to 1-day old adults for wild-type and between *unc-54::A β ₁₋₄₂* animals shifted from 20°C to the higher permissive 25°C temperature (after A β -induction). As expected, the fold-change ratio of circ-*crh-1* gene expression was higher in *unc-54::A β ₁₋₄₂* animals than wild-type by 1.25-fold (Figure 2A). Importantly, expression of linear *crh-1* was not significantly affected after A β -induction in 1-day and 4-day old adults (Figure 2A). Similar results were observed when normalizing circ-*crh-1* gene expression of 4-day old *unc-54::A β ₁₋₄₂* adults at 25°C (after A β -induction) to the 20°C temperature (before A β -induction) (Figure 2B). These results suggest that A β -induction positively regulates circ-*crh-1* expression, consistent with a detrimental role for age-accumulated circRNAs in AD.

3.4 Loss of circ-*crh-1* expression reduces A β -aggregation

Next, we asked whether loss of circ-*crh-1* expression reduced A β -aggregate deposits in *unc-54::A β ₁₋₄₂* animals, which results in age-progressive paralysis and a shortened lifespan (Figure 1). In order to rule out the effects of circ-*crh-1* loss on the transcription of A β ₁₋₄₂ expression rather than simply reducing A β aggregates in muscle, we first used RT-qPCR analysis to measure A β mRNA levels at different aging time-points. We found no significant differences in A β gene expression between *unc-54::A β ₁₋₄₂* and *crh-1(syb385); unc-54::A β ₁₋₄₂* animals at 1, 2, and 3-day old adulthood at the higher permissive 25°C temperature (Figure 3A). We then utilized the sensitive amyloid-binding dye X-34 (Link et al., 2001) to specifically stain and visualize *in vivo* A β aggregates in muscle cells of *C. elegans* as reported (McColl et al., 2012) and assessed whether circ-*crh-1(-)* mutations reduce the number of A β aggregates puncta in *unc-54::A β ₁₋₄₂* expressing worms. Consistent with the delayed onset of the age-progressive A β -induced paralysis and restoration of the shortened lifespan, we found that the number of X-34 positive A β -aggregates were significantly reduced (*p* < 0.05) in *crh-1(syb385)* mutants carrying *unc-54::A β ₁₋₄₂* compared to GMC101 in 5-day old adults at the higher permissive 25°C temperature (Figures 3B, C). Thus, loss of circ-*crh-1* expression inhibits the accumulation of A β aggregates.

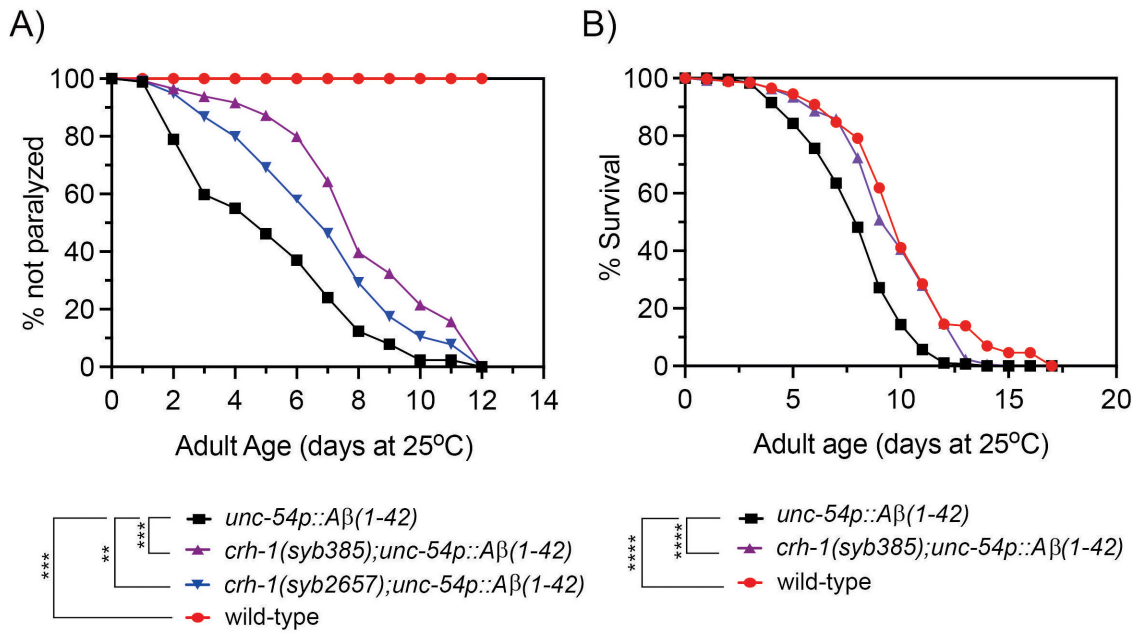


FIGURE 1

Loss of circ-*crh-1* delays paralysis and decreases the short lifespan of an Aβ-induced proteotoxicity model. **(A)** The onset of paralysis measured in the Aβ-proteotoxicity model strain, GMC101 (*unc-54p::Aβ₁₋₄₂*) and the GMC101 strain carrying either a *syb385* mutation (purple) or *syb2657* mutation (blue) after a temperature upshift from 20°C to 25°C. Wild-type (red) or *unc-54p::Aβ₁₋₄₂* (GMC101, black) animals at 20°C do not show paralysis. 3 independent trials with $n > 140$ animals for each assay and genotype in the presence of 0.5 μM FUDR. Asterisks indicate statistical significance with $**p < 0.01$, $***p < 0.001$. **(B)** Lifespan curves for *unc-54p::Aβ₁₋₄₂* (GMC101) animals compared to *crh-1(syb385); unc-54p::Aβ₁₋₄₂* and wild-type animals at 25°C. Induction of *unc-54p::Aβ₁₋₄₂* shortens lifespan compared to wild-type ($****p < 0.0001$, Mantel-Cox log-rank test), which can be reversed by *syb385* mutations. There is a non-significant difference in mean lifespan between *crh-1(syb385); unc-54p::Aβ₁₋₄₂* and wild-type ($p < 0.035$, Mantel-Cox log-rank test). See [Supplementary Table 3](#) for lifespan statistics. $n = 3-4$ independent lifespan assays were performed with $n = 90-150$ animals for each assay and genotype in the presence of 0.5 μM FUDR (see section “2 Materials and methods”).

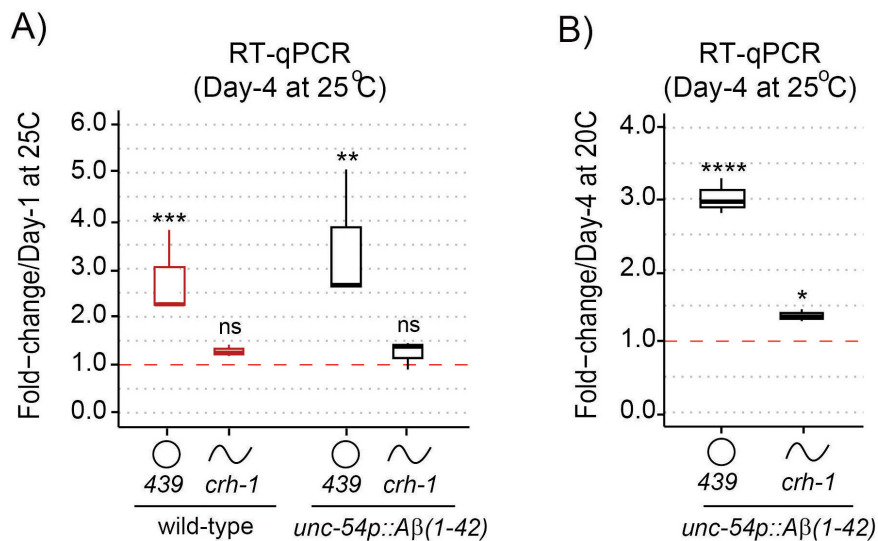


FIGURE 2

circ-*crh-1* expression is increased after Aβ-induction during aging. **(A)** RT-qPCR expression of the abundant circular circ-*crh-1* (*cel_circ_0000439*) and linear *crh-1* transcripts in 4-day adults normalized to 1-day adults of wild-type and *unc-54p::Aβ₁₋₄₂* (GMC101) at 25°C. **(B)** RT-qPCR expression of circular and linear *crh-1* transcripts in day-4 adults of *unc-54p::Aβ₁₋₄₂* (GMC101) at 25°C (after Aβ-induction) normalized to 1-day adults of *unc-54p::Aβ₁₋₄₂* (GMC101) at 20°C (no Aβ-induction). circ-*crh-1* expression increases after induction of Aβ. $n = 3$ independent biological samples for both panels **(A)** and **(B)**. For RT-qPCR expression analysis, data in panels **(A)** and **(B)** was normalized to *cdc-42* mRNA. Data is represented as mean ± SEM. ns, not significant. $*p < 0.05$, $**p < 0.01$, $***p < 0.001$, $****p < 0.0001$.

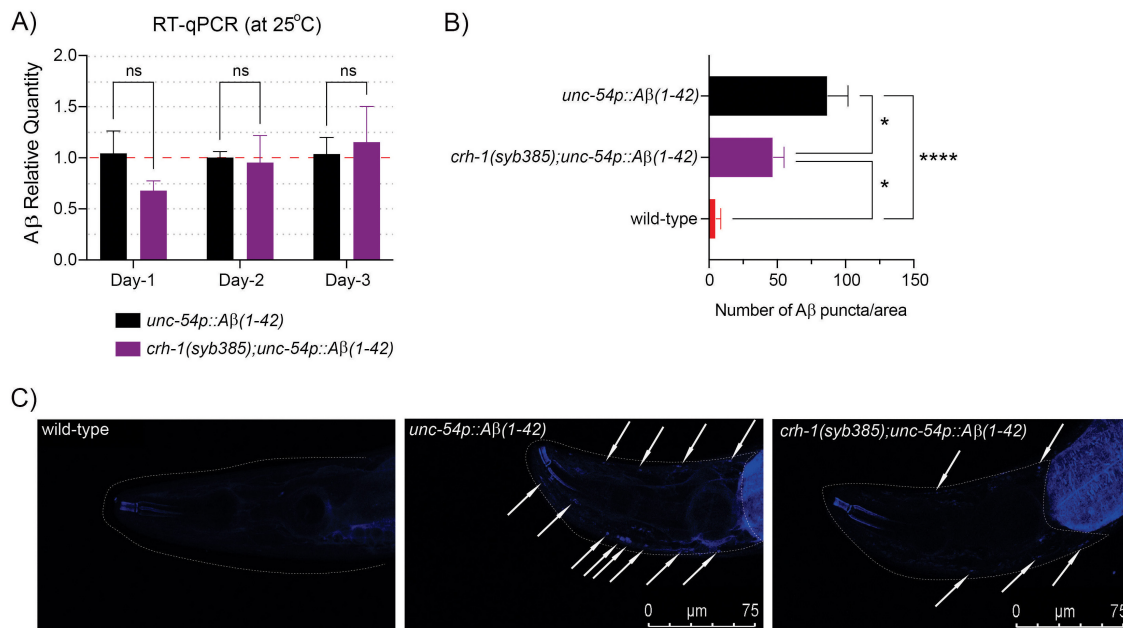


FIGURE 3 *circ-crh-1* mutation reduces Aβ-aggregation. **(A)** Relative quantity of Aβ₁₋₄₂ gene expression in *unc-54p::Aβ₁₋₄₂* (GMC101, black), *crh-1(syb385);unc-54p::Aβ₁₋₄₂* (purple) animals during aging (1-day, 2-day, and 3-day old adults at 25°C) as determined by RT-qPCR. Data is represented as mean ± SEM and was normalized to *cdc-42* mRNA. *n* = 3 independent biological samples, ns, not significant. **(B)** Quantitative analysis of Aβ₁₋₄₂ deposits in the head region of wild-type (red), *unc-54p::Aβ₁₋₄₂* (GMC101, black), and *crh-1(syb385);unc-54p::Aβ₁₋₄₂* (purple) animals. The quantity is expressed as mean number ± SEM of Aβ deposits/area of the head region. *n* = 10 animals per genotype. **p* < 0.05, *****p* < 0.0001. **(C)** Representative images of X-34 staining in wild-type (left), *unc-54p::Aβ₁₋₄₂* (GMC101, middle) and *crh-1(syb385);unc-54p::Aβ₁₋₄₂* (right) animals. White arrows indicate Aβ₁₋₄₂ reactive deposits (arrows) in the worm head (dotted white line). Scale bar represents 75 μm.

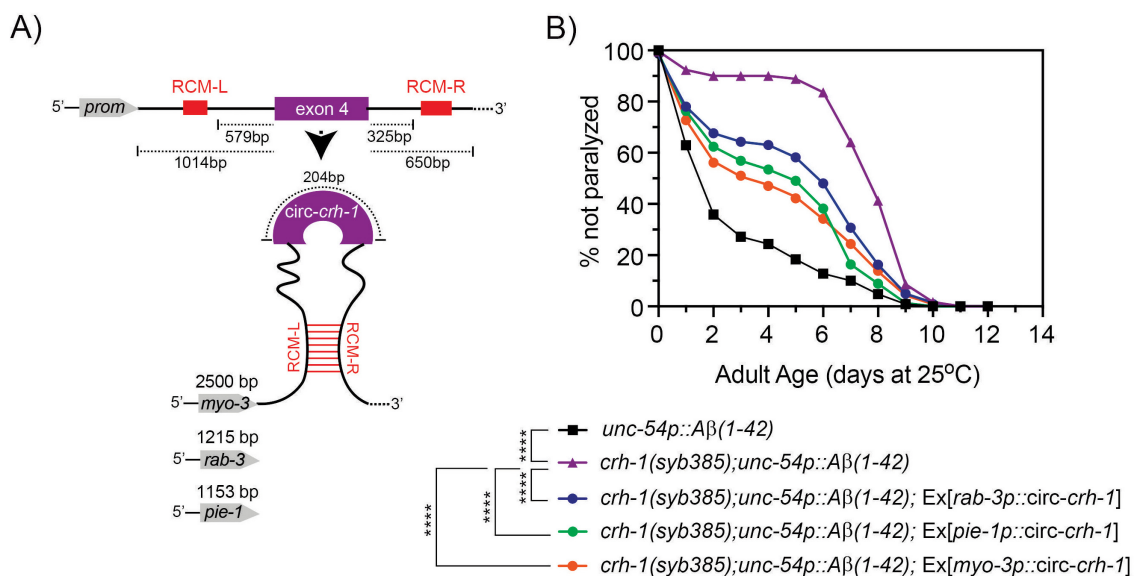


FIGURE 4 Expression of *circ-crh-1* in multiple tissues can partially rescue the delayed onset of Aβ-induced paralysis in *circ-crh-1* mutants. **(A)** Schematic of plasmid-based minigene used to overexpress *circ-crh-1* under control of tissue-defined promoters. Shown is the *crh-1*(exon4) and reverse complementary match sequences (RCM-L and RCM-R) predicted to facilitate back-splicing of *circ-crh-1*. Promoters and lengths used are *myo-3* with 2,500 bp for muscle expression, *rab-3* with 1,215 bp for pan-neural expression, and *pie-1* with 1,153 bp for germline expression. **(B)** Paralysis measured in *crh-1(syb385);unc-54p::Aβ₁₋₄₂* animals overexpressing *circ-crh-1* in *myo-3*-expressing muscle cells, *rab-3*-expressing neurons, and *pie-1*-expressing germline cells compared to *unc-54p::Aβ₁₋₄₂* (GMC101, black), *crh-1(syb385);unc-54p::Aβ₁₋₄₂* (purple) animals after a temperature upshift from 20°C to 25°C. 3 independent trials with *n* > 140 animals for each assay in the presence of 0.5 μM FUDR. Asterisks indicate statistical significance with *****p* < 0.0001.

3.5 circ-*crh-1* expression is required in muscle for A β -induced paralysis

We next asked whether circ-*crh-1* expression in muscle could restore the delayed onset of A β -induced paralysis of *crh-1(syb385)* mutants expressing A β_{1-42} in muscle cells. To investigate this question, we used tissue-specific rescue experiments. We previously showed that circ-*crh-1* expression in neurons is an important determinant for lifespan regulation (Knupp et al., 2022). We decided to create *crh-1(syb385); unc-54::A β_{1-42}* transgenic animals that express circ-*crh-1* under select tissue-specific promoters. We cloned the *crh-1*(exon 4) circularizing sequence in between the left and right reverse complementary match (RCM) sequences, and used muscle (*myo-3*), pan-neural (*rab-3*), or germline (*pie-1*) specific promoters to drive the circ-*crh-1* expression transgene (Figure 4A). Expression of circ-*crh-1* under control of the muscle-specific *myo-3* promoter could partially restore the delayed onset of A β -induced paralysis of *crh-1(syb385); unc-54::A β_{1-42}* animals at the higher permissive 25°C temperature (Figure 4B), suggesting that circ-*crh-1* expression in muscle is an important determinant for A β -induced toxicity. Surprisingly, however, circ-*crh-1* expression driven by *rab-3* and *pie-1* promoters also partially restored A β -induced paralysis at 25°C (Figure 4B). These results suggest that in addition to muscle, circ-*crh-1* expression may have additional requirements in other tissues to alter A β -induced paralysis.

3.6 The delayed onset of A β -induced paralysis in circ-*crh-1* mutants is dependent on *col-49* expression

We previously showed that circ-*crh-1(-)* mutants exhibit widespread transcriptomic changes that might impact various age-related pathways (Cortés-López et al., 2018). Notably, among the identified genes, a subset included collagen-encoding genes with many of which showed increased expression levels in circ-*crh-1(-)* mutants. Interestingly, cuticular collagens are implicated in A β aggregate formation and clearance pathways of A β in *C. elegans* (Jongsma et al., 2023). We hypothesized that the increased expression of cuticular collagen genes contributes to the amelioration of A β -induced toxicity in circ-*crh-1(-)* mutants carrying the *unc-54::A β_{1-42}* transgene. To test this hypothesis, we selected six cuticular collagen genes of interest from the 21 collagen genes with elevated expression previously identified in *crh-1(syb385)* mutants (Knupp et al., 2022), including collagens that have a known association with lifespan such as *col-49* and *col-179* (Palani et al., 2023). Among the collagen genes tested by RT-qPCR analysis, only *col-49* showed elevated gene expression levels in *crh-1(syb385)* mutants expressing *unc-54::A β_{1-42}* compared to GMC101 controls at 25°C in 3-day old adults (Figure 5A). No detectable differences were observed in total collagen levels in *crh-1(syb385)* mutants compared to wild-type under different cultivation temperatures (Supplementary Figure 2). Thus, the elevated expression of *col-49* in *crh-1(syb385)* mutants likely represents a specific response to A β -induced toxicity, rather than a

general increase in collagen production driven by circ-*crh-1*.

We next generated *col-49* deletion mutants using a CRISPR/Cas9 strategy and crossed the mutant with GMC101 to assess A β -induced toxicity through a paralysis assay at 25°C. We found that *col-49(syb8747); unc-54::A β_{1-42}* animals exhibited an exacerbated, age-progressive paralysis compared to the control (GMC101) at the higher 25°C permissive temperature (Figure 5B). *col-49(syb8747)* mutants without the *unc-54::A β_{1-42}* transgene did not display paralysis at 25°C (Figure 5B).

To test whether *col-49* expression is required for the delayed onset of A β -induced toxicity observed in *crh-1(syb385)* mutants, we crossed the *col-49(syb8747)* mutation into *crh-1(syb385)* mutants, both of which carried the *unc-54::A β_{1-42}* transgene. Mutations in *col-49(syb8747)* significantly suppressed the delayed A β -induced paralysis phenotype of *crh-1(syb385)* animals with the *unc-54::A β_{1-42}* transgene when 1-day old adults were shifted from 20°C to the higher 25°C permissive temperature (Figure 6A). We also examined overexpression (OE) of *col-49* on A β -induced paralysis, and found that *col-49* OE transgenic animals weakly but significantly ($p < 0.05$) delayed the onset of A β -induced paralysis (Figure 6B) similar as circ-*crh-1(-)* mutants. Collectively, these results suggest that *col-49* gene expression is elevated in circ-*crh-1(-)* mutants, and that loss of circ-*crh-1* promotes A β -induced paralysis in a *col-49* dependent manner.

4 Discussion

The expression of circRNAs accumulate during aging in *C. elegans*, *Drosophila* and mice (Westholm et al., 2014; Gruner et al., 2016; Hall et al., 2017; Cortés-López et al., 2018) as well as in age-associated disorders such as Alzheimer's disease (AD) (Dube et al., 2019), but the role of age-accumulated circRNAs in AD remains unclear. We assessed whether loss of a single abundant and age-accumulated circRNA, called circ-*crh-1*, could protect against amyloid β -induced toxicity using a well-established *C. elegans* transgenic strain that expresses human A β_{1-42} in muscle cells, which results in age-progressive full body paralysis and shortened lifespan. We found a significant delay in the onset of A β -induced paralysis in two independent circ-*crh-1(-)* mutants, which could partially be rescued by re-introducing circ-*crh-1* expression in muscle, neurons and germline cells. In addition, we observed that circ-*crh-1(-)* mutants improve the reduced lifespan of muscle expressing A β_{1-42} animals. We further demonstrated that genetic removal of circ-*crh-1* expression results in a reduction of A β aggregates, suggesting that loss of a single age-accumulated circRNA protects against the age-related onset of A β toxicity in *C. elegans*.

Our transgenic experiments implicate circ-*crh-1* expression in muscle by which circ-*crh-1* could delay the onset of A β_{1-42} -induced paralysis in the GMC101 strain. We also observed that circ-*crh-1* expression in neurons and germline cells could partially restore the delayed onset of A β_{1-42} -induced paralysis caused by

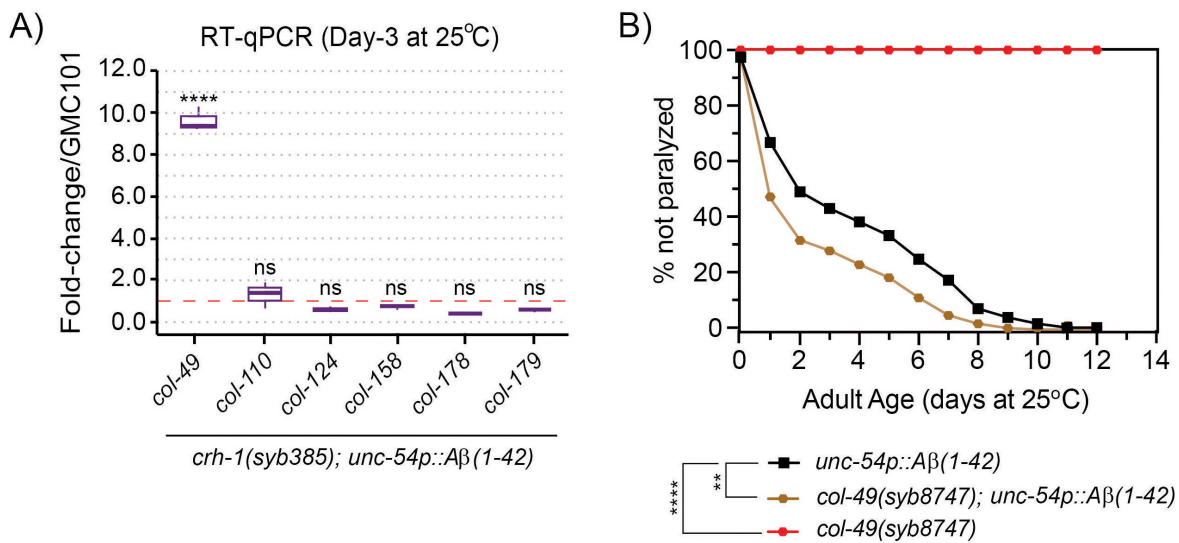


FIGURE 5 circ-*crh-1* mutations increase *col-49* expression after Aβ-induction, whereas loss of *col-49* promotes Aβ-induced paralysis. **(A)** RT-qPCR expression of 6 predicted cuticular collagen genes in *crh-1(syb385); unc-54p::Aβ₁₋₄₂* (after Aβ-induction) in 3-day old adults. *col-49* expression is strongly increased after Aβ-induction in *crh-1(syb385)* mutants. Data is represented as mean ± SEM and was normalized to *act-1* mRNA. *n* = 3 independent biological samples. ns, not significant. *****p* < 0.0001. **(B)** Paralysis measured in *unc-54p::Aβ₁₋₄₂* animals carrying a *col-49(syb8747)* mutation (brown) compared to *unc-54p::Aβ₁₋₄₂* (GMC101, black) and *col-49(syb8747)* mutant animals (red). The *syb8747* allele has a 1,180 bp deletion generated by CRISPR/Cas9 (see section “2 Materials and methods”). 3 independent trials with *n* > 140 animals for each assay in the presence of 0.5 μM FUDR. Asterisks indicate statistical significance with ***p* < 0.01 and *****p* < 0.0001.

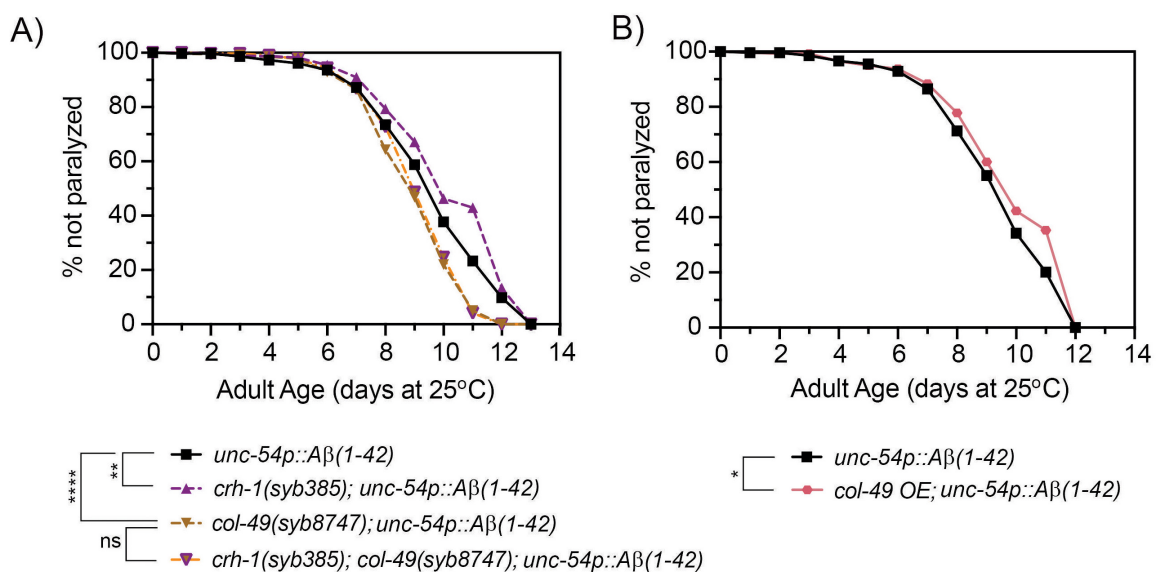


FIGURE 6 A mutation in *col-49* suppresses the delayed Aβ-induced paralysis of circ-*crh-1* mutants, while *col-49* overexpression reduces Aβ-induced paralysis. **(A)** Paralysis measured in *unc-54p::Aβ₁₋₄₂* animals carrying both *col-49(syb8747)* and *crh-1(385)* mutations (orange line with purple triangle) compared to *unc-54p::Aβ₁₋₄₂* (GMC101, black), *col-49(syb8747); unc-54p::Aβ₁₋₄₂* (light brown) and *crh-1(syb385); unc-54p::Aβ₁₋₄₂* mutant animals (purple). **(B)** Paralysis measured in transgenic animals overexpressing (OE) the *col-49* gene (salmon) compared to *unc-54p::Aβ₁₋₄₂* animals (GMC101, black). **(A, B)** In these experiments, 1-day old adults were upshifted from the non-restrictive 20°C temperature to the higher permissive 25°C temperature to induce paralysis by Aβ. 3 independent trials with *n* > 100 animals for each assay in the presence of 0.5 μM FUDR. ns, not significant. Asterisks indicate statistical significance with **p* < 0.05, ***p* < 0.01 and *****p* < 0.0001 (Mantel-Cox log-rank test).

circ-*crh-1* mutations. The GMC101 strain is an inducible model for muscle expressing Aβ₁₋₄₂ aggregation and proteotoxicity (McColl et al., 2012). Aβ peptides can spread and transfer between cells (Domert et al., 2014). In *C. elegans*, intracellular

Aβ₁₋₄₂ peptides expressed in a subset of neurons are able to spread to other cells and distal tissues, and targeted depletion of neuronal Aβ can systemically delay Aβ aggregation (Gallrein et al., 2021). Our rescue experiments suggest that circ-*crh-1*

expression is required in other tissues besides muscle for A β _{1–42}-induced paralysis, but it remains uncertain whether the GMC101 strain exhibits systemic defects and aggregation of A β _{1–42} beyond the tissue of expression (i.e., muscle). It might also be possible that overexpression of circ-*crh-1* in neurons and germline cells leads to non-cell-autonomous rescue of muscle expressing A β _{1–42} aggregates (Nussbaum-Krammer and Morimoto, 2014). Further experiments demonstrating *in vivo* expression of circ-*crh-1* coupled with labeling A β _{1–42} could offer insight into the mechanisms through which circ-*crh-1* regulates A β _{1–42} aggregation and its phenotypic consequences.

Using transcriptome-wide analysis, we previously showed increased expression of multiple collagen-encoding genes in circ-*crh-1*(-) mutants (Knupp et al., 2022). Collagens have previously been linked to Alzheimer's disease, with several collagens influencing A β -aggregate formation (Cheng et al., 2009; Tong et al., 2010). Moreover, a recent study reported that *C. elegans* cuticular collagens are implicated in extracellular A β -aggregate formation and clearance (Jongsma et al., 2023). We selected 6 collagen genes with elevated expression in circ-*crh-1*(-) mutants (Knupp et al., 2022) and tested them in circ-*crh-1*(-) mutants expressing A β _{1–42} in muscle. We found that expression levels of the predicted cuticular collagen, *col-49*, with a known role in lifespan regulation (Palani et al., 2023) and cuticular integrity (Jackson et al., 2014) was significantly increased, while the other tested collagen genes were not different from the GMC101 control. We do not yet know how loss of circ-*crh-1* expression results in increased *col-49* mRNA levels in the presence of muscle expressing A β _{1–42}. We favor the possibility that circ-*crh-1* interacts with RNA-binding proteins (RBPs) to regulate their expression and function by acting as a sponge, decoy, scaffold or recruiter, which could affect the fate of mRNA targets of RBPs through post-transcriptional processes (Patop et al., 2019; Chen, 2020). In this scenario, and consistent with loss of circ-*crh-1* expression resulting in transcriptomic changes (Knupp et al., 2022), circ-*crh-1* may sequester away RBPs from *col-49* mRNA targets, which in turn alters its expression.

Collagen biosynthesis and stability in *C. elegans* can affect A β -aggregate levels (Jongsma et al., 2023). While we did not observe any changes in overall collagen levels in whole circ-*crh-1*(-) mutant animals, we found that mutants lacking *col-49* exacerbate the A β _{1–42}-induced paralysis. This exacerbation might be explained by circ-*crh-1* indirectly modulating *col-49* mRNA levels through one or more yet unidentified RBPs, thereby altering A β -induced toxicity. Consistent with this hypothesis, our findings show that *col-49* expression is elevated in circ-*crh-1*(-) mutants. We further demonstrated that the delayed onset of A β -induced paralysis observed in circ-*crh-1*(-) mutants is dependent on *col-49* expression, as mutations in *col-49* can suppress the delayed onset of A β -induced paralysis of circ-*crh-1* mutants. Further research on identifying the specific RBP(s) that interact with circ-*crh-1* could provide crucial insights into the regulatory mechanisms by which the loss of circ-*crh-1* promotes A β _{1–42}-induced paralysis.

In conclusion, our study shows that the expression of *crh-1* circRNAs is important for modulating A β -induced toxicity in Alzheimer's disease (AD) and could pave the

way for using *C. elegans* to study circRNAs in AD and its relationship to aging.

Data availability statement

The original contributions presented in this study are included in this article/Supplementary material, further inquiries can be directed to the corresponding author.

Ethics statement

The manuscript presents research on animals that do not require ethical approval for their study.

Author contributions

HA: Conceptualization, Formal Analysis, Investigation, Methodology, Validation, Visualization, Writing – original draft, Writing – review and editing. TB: Formal Analysis, Investigation, Methodology, Validation, Visualization, Writing – review and editing. ER: Formal Analysis, Investigation, Methodology, Validation, Visualization, Writing – review and editing. AL: Conceptualization, Data curation, Formal Analysis, Funding acquisition, Investigation, Methodology, Project administration, Resources, Software, Supervision, Validation, Visualization, Writing – original draft, Writing – review and editing.

Funding

The author(s) declare that financial support was received for the research and/or publication of this article. This work was supported by the National Institutes of Health grants R21 AG058955 (to AL) and R01 NS107969 (to AL). Research reported in this study utilized the COBRE Cellular and Molecular Imaging Core facility at the University of Nevada, Reno, which is supported by the National Institutes of Health grant P30 GM145646. Some strains were provided by the CGC, which is funded by NIH Office of Research Infrastructure Programs P40 OD010440.

Acknowledgments

We thank members of the van der Linden for useful discussions and feedback on the manuscript, SunyBiotech for help with cloning the *myo-3p::circ-crh-1* construct, as well as creating transgenic lines and mutants, and the Cellular and Molecular Imaging (CMI) Core facility at the University of Nevada, supported by a grant from the NIH National Institutes of General Medical Sciences (P30 GM145646), for providing equipment and resources. We also thank the Caenorhabditis Genetics Center (CGC), funded by the NIH Office of Research Infrastructure Programs (P40 OD010440), for

providing strains used in this study. This study appeared as a pre-print in BioRxiv (Alshareef et al., 2024).

Conflict of interest

The authors declare that the research was conducted in the absence of any commercial or financial relationships that could be construed as a potential conflict of interest.

Publisher's note

All claims expressed in this article are solely those of the authors and do not necessarily represent those of their affiliated organizations, or those of the publisher, the editors and the reviewers. Any product that may be evaluated in this article, or claim that may be made by its manufacturer, is not guaranteed or endorsed by the publisher.

References

- Alshareef, H., Ballinger, T., Rojas, E., and Van Der Linden, A. M. (2024). Loss of age-accumulated crh-1 circRNAs ameliorate amyloid β -induced toxicity in a C. Elegans model for Alzheimer's disease. *bioRxiv [Preprint]* doi: 10.3389/fnagi.2025.1464015
- Beylerli, O., Beilerli, A., Ilyasova, T., Shumadalova, A., Shi, H., and Sufianov, A. (2024). CircRNAs in Alzheimer's disease: What are the prospects? *Noncoding RNA Res.* 9, 203–210. doi: 10.1016/j.ncrna.2023.11.011
- Brenner, S. (1974). The genetics of Caenorhabditis elegans. *Genetics* 77, 71–94. doi: 10.1093/genetics/77.1.71
- Chen, L. (2020). The expanding regulatory mechanisms and cellular functions of circular RNAs. *Nat. Rev. Mol. Cell. Biol.* 21, 475–490. doi: 10.1038/s41580-020-0243-y
- Cheng, J., Dubal, D., Kim, D., Legleiter, J., Cheng, I., Yu, G., et al. (2009). Collagen VI protects neurons against Abeta toxicity. *Nat. Neurosci.* 12, 119–121. doi: 10.1038/nn.2240
- Cortés-López, M., Gruner, M., Cooper, D., Gruner, H., Voda, A., van der Linden, A., et al. (2018). Global accumulation of circRNAs during aging in Caenorhabditis elegans. *BMC Genomics* 19:8. doi: 10.1186/s12864-017-4386-y
- Domert, J., Rao, S., Agholme, L., Brorsson, A., Marcusson, J., Hallbeck, M., et al. (2014). Spreading of amyloid- β peptides via neuritic cell-to-cell transfer is dependent on insufficient cellular clearance. *Neurobiol. Dis.* 65, 82–92. doi: 10.1016/j.nbd.2013.12.019
- Dube, U., Del-Aguila, J., Li, Z., Budde, J., Jiang, S., Hsu, S., et al. (2019). An atlas of cortical circular RNA expression in Alzheimer disease brains demonstrates clinical and pathological associations. *Nat. Neurosci.* 22, 1903–1912. doi: 10.1038/s41593-019-0501-5
- Fay, D. (2006). Genetic mapping and manipulation: Chapter 1—Introduction and basics. *WormBook* 1–12. doi: 10.1895/wormbook.1.90.1
- Gallrein, C., Iburg, M., Michelberger, T., Koçak, A., Puchkov, D., Liu, F., et al. (2021). Novel amyloid-beta pathology C. elegans model reveals distinct neurons as seeds of pathogenicity. *Prog. Neurobiol.* 198:101907. doi: 10.1016/j.pneurobio.2020.101907
- Gruner, H., Cortés-López, M., Cooper, D., Bauer, M., and Miura, P. (2016). CircRNA accumulation in the aging mouse brain. *Sci. Rep.* 6:38907. doi: 10.1038/srep38907
- Hall, H., Medina, P., Cooper, D., Escobedo, S., Rounds, J., Brennan, K., et al. (2017). Transcriptome profiling of aging Drosophila photoreceptors reveals gene expression trends that correlate with visual senescence. *BMC Genomics* 18:894. doi: 10.1186/s12864-017-4304-3
- Han, S., Lee, D., Lee, H., Kim, D., Son, H., Yang, J., et al. (2016). OASIS 2: Online application for survival analysis 2 with features for the analysis of maximal lifespan and healthspan in aging research. *Oncotarget* 7, 56147–56152. doi: 10.18632/oncotarget.11269
- Hansen, T., Jensen, T., Clausen, B., Bramsen, J., Finsen, B., Damgaard, C., et al. (2013). Natural RNA circles function as efficient microRNA sponges. *Nature* 495, 384–388. doi: 10.1038/nature11993
- Jackson, B., Abete-Luzi, P., Krause, M., and Eisenmann, D. (2014). Use of an activated beta-catenin to identify Wnt pathway target genes in caenorhabditis elegans, including a subset of collagen genes expressed in late larval development. *G3 (Bethesda)* 4, 733–747. doi: 10.1534/g3.113.009522
- Jeck, W., Sorrentino, J., Wang, K., Slevin, M., Burd, C., Liu, J., et al. (2013). Circular RNAs are abundant, conserved, and associated with ALU repeats. *RNA* 19, 141–157. doi: 10.1261/rna.035667.112
- Jongsma, E., Goyal, A., Mateos, J., and Ewald, C. (2023). Removal of extracellular human amyloid beta aggregates by extracellular proteases in C. elegans. *Elife* 12:e83465. doi: 10.7554/eLife.83465
- Kim, E., Kim, Y., and Lee, S. (2021). Emerging functions of circular RNA in aging. *Trends Genet.* 37, 819–829. doi: 10.1016/j.tig.2021.04.014
- Knupp, D., and Miura, P. (2018). CircRNA accumulation: A new hallmark of aging? *Mech. Ageing Dev.* 173, 71–79. doi: 10.1016/j.mad.2018.05.001
- Knupp, D., Jorgensen, B., Alshareef, H., Bhat, J., Grubbs, J., Miura, P., et al. (2022). Loss of circRNAs from the crh-1 gene extends the mean lifespan in Caenorhabditis elegans. *Aging Cell.* 21:e13560. doi: 10.1111/acer.13560
- Li, X., Yang, L., and Chen, L. (2018). The biogenesis, functions, and challenges of circular RNAs. *Mol. Cell.* 71, 428–442. doi: 10.1016/j.molcel.2018.06.034
- Link, C., Johnson, C., Fonte, V., Paupard, M., Hall, D., Styren, S., et al. (2001). Visualization of fibrillar amyloid deposits in living, transgenic Caenorhabditis elegans animals using the sensitive amyloid dye, X-34. *Neurobiol. Aging* 22, 217–226. doi: 10.1016/s0197-4580(00)00237-2
- McColl, G., Roberts, B., Pukala, T., Kenche, V., Roberts, C., Link, C., et al. (2012). Utility of an improved model of amyloid-beta ($A\beta$ 1–42) toxicity in Caenorhabditis elegans for drug screening for Alzheimer's disease. *Mol. Neurodegener.* 7:57. doi: 10.1186/1750-1326-7-57
- Nussbaum-Krammer, C., and Morimoto, R. (2014). Caenorhabditis elegans as a model system for studying non-cell-autonomous mechanisms in protein-misfolding diseases. *Dis. Model. Mech.* 7, 31–39. doi: 10.1242/dmm.013011
- Palani, S., Sellegounder, D., Wibisono, P., and Liu, Y. (2023). The longevity response to warm temperature is neurally controlled via the regulation of collagen genes. *Aging Cell.* 22:e13815. doi: 10.1111/acer.13815
- Patop, I., Wüst, S., and Kadener, S. (2019). Past, present, and future of circRNAs. *EMBO J.* 38:e100836. doi: 10.15252/embj.2018100836
- Shi, Z., Chen, T., Yao, Q., Zheng, L., Zhang, Z., Wang, J., et al. (2017). The circular RNA ciRS-7 promotes APP and BACE1 degradation in an NF- κ B-dependent manner. *FEBS J.* 284, 1096–1109. doi: 10.1111/febs.14045
- Sun, F., Zhang, Y., Wu, X., Xu, X., Zhu, C., and Huang, W. (2023). Brevescapine combined with BMSCs reduces $A\beta$ deposition in rat with Alzheimer's disease by regulating circular RNA ciRS-7. *Curr. Mol. Med.* 23, 76–86. doi: 10.2174/1566524022666220113151044

Supplementary material

The Supplementary Material for this article can be found online at: <https://www.frontiersin.org/articles/10.3389/fnagi.2025.1464015/full#supplementary-material>

SUPPLEMENTARY FIGURE 1

Lifespan analysis of GMC101 at 20°C. Lifespan curve for *unc-54p::A β 1–42* (GMC101) animals compared to wild-type animals at 20°C. There is a non-significant difference in mean lifespan between *unc-54p::A β 1–42* and wild-type controls ($p = 0.642$, Mantel-Cox log-rank test). See [Supplementary Table 3](#) for lifespan statistics. $n = 4$ independent lifespan assays were performed with $n = 90$ –120 animals for each assay and genotype in the presence of 0.5 μ M FUDR (see section “2 Materials and methods”).

SUPPLEMENTARY FIGURE 2

Total collagen in *circ-crh-1* mutants at different temperatures. Total collagen-to-protein ratio in *crh-1(syb385)* mutants compared to wild-type for 1-day adult worms at 15°C, 20°C, and 25°C. There is a non-significant difference in mean total collagen level between *crh-1(syb385)* mutants and wild-type animals (15°C, $p = 0.423$; 20°C, $p = 0.632$; 25°C, $p = 0.250$). $n = 3$ independent total collagen determination assays.

Teuscher, A., Statzer, C., Pantasis, S., Bordoli, M., and Ewald, C. (2019). Assessing collagen deposition during aging in mammalian tissue and in *Caenorhabditis elegans*. *Methods Mol. Biol.* 1944, 169–188. doi: 10.1007/978-1-4939-9095-5_13

Tong, Y., Xu, Y., Scearce-Levie, K., Ptáček, L., and Fu, Y. (2010). COL25A1 triggers and promotes Alzheimer's disease-like pathology in vivo. *Neurogenetics* 11, 41–52. doi: 10.1007/s10048-009-0201-5

Weigelt, C., Sehgal, R., Tain, L., Cheng, J., Eßer, J., Pahl, A., et al. (2020). An insulin-sensitive circular RNA that regulates lifespan in *Drosophila*. *Mol. Cell* 79, 268–279.e5. doi: 10.1016/j.molcel.2020.06.011.

Westholm, J., Miura, P., Olson, S., Shenker, S., Joseph, B., Sanfilippo, P., et al. (2014). Genome-wide analysis of drosophila circular RNAs reveals their structural and sequence properties and age-dependent neural accumulation. *Cell. Rep.* 9, 1966–1980. doi: 10.1016/j.celrep.2014.10.062

Zhang, N., Gao, Y., Yu, S., Sun, X., and Shen, K. (2020). Berberine attenuates A β 42-induced neuronal damage through regulating circHDAC9/miR-142-5p axis in human neuronal cells. *Life Sci.* 252:117637. doi: 10.1016/j.lfs.2020.117637

Zhang, X., Wang, H., Zhang, Y., Lu, X., Chen, L., and Yang, L. (2014). Complementary sequence-mediated exon circularization. *Cell* 159, 134–147. doi: 10.1016/j.cell.2014.09.001